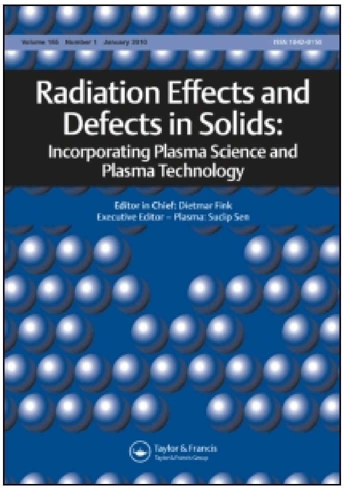

Radiation Effects and Defects in Solids
Publication details, including instructions for authors and subscription information:
http://www.informaworld.com/smpp/title~content=t713648881

A self-injection acceleration test experiment for the FLAME laser

L. Labate[abc]; F. Anelli[c]; A. Bacci[d]; D. Batani[de]; M. Bellaveglia[c]; C. Benedetti[fg]; R. Benocci[de]; L. Cacciotti[c]; C. A. Cecchetti[ab]; O. Ciricosta[abh]; A. Clozza[c]; L. Cultrera[c]; G. Di Pirro[c]; N. Drenska[ij]; R. Faccini[ij]; M. Ferrario[c]; D. Filippetto[c]; S. Gallo[c]; S. Fioravanti[c]; A. Gamucci[ab]; G. Gatti[c]; A. Ghigo[c]; A. Giulietti[ab]; D. Giulietti[abch]; P. Köster[ab]; T. Levato[ac]; V. Lollo[c]; E. Pace[c]; N. Pathak[ah]; A. Rossi[ad]; L. Serafini[cd]; G. Turchetti[fg]; C. Vaccarezza[c]; P. Valente[ij]; C. Vicario[c]; L. A. Gizzi[abc]

[a] Intense Laser Irradiation Laboratory, INO, CNR, Pisa, Italy [b] INFN, Sezione di Pisa, Italy [c] Laboratori Nazionali di Frascati, INFN, Italy [d] INFN, Sezione di Milano, Italy [e] Dipartimento di Fisica, Università di Milano-Bicocca, Italy [f] Dipartimento Fisica, Università di Bologna, Italy [g] INFN, Sezione di Bologna, Italy [h] Dipartimento Fisica, Università di Pisa, Italy [i] Dipartimento Fisica, Università di Roma “La Sapienza”, Italy [j] INFN, Italy

To cite this Article Labate, L. , Anelli, F. , Bacci, A. , Batani, D. , Bellaveglia, M. , Benedetti, C. , Benocci, R. , Cacciotti, L. , Cecchetti, C. A. , Ciricosta, O. , Clozza, A. , Cultrera, L. , Di Pirro, G. , Drenska, N. , Faccini, R. , Ferrario, M. , Filippetto, D. , Gallo, S. , Fioravanti, S. , Gamucci, A. , Gatti, G. , Ghigo, A. , Giulietti, A. , Giulietti, D. , Köster, P. , Levato, T. , Lollo, V. , Pace, E. , Pathak, N. , Rossi, A. , Serafini, L. , Turchetti, G. , Vaccarezza, C. , Valente, P. , Vicario, C. and Gizzi, L. A.(2010) 'A self-injection acceleration test experiment for the FLAME laser', Radiation Effects and Defects in Solids, 165: 6, 787 — 793

To link to this Article: DOI: 10.1080/10420151003732056

URL: http://dx.doi.org/10.1080/10420151003732056

Radiation Effects & Defects in Solids: Incorporating Plasma Science & Plasma Technology
Vol. 165, Nos. 6–10, June–October 2010, 787–793

A self-injection acceleration test experiment for the FLAME laser

L. Labate[a,b,c]*, F. Anelli[c], A. Bacci[d], D. Batani[d,e], M. Bellaveglia[c], C. Benedetti[f,g], R. Benocci[d,e], L. Cacciotti[c], C.A. Cecchetti[a,b], O. Ciricosta[a,b,h], A. Clozza[c], L. Cultrera[c], G. Di Pirro[c], N. Drenska[i,j], R. Faccini[i,j], M. Ferrario[c], D. Filippetto[c], S. Gallo[c], S. Fioravanti[c], A. Gamucci[a,b], G. Gatti[c], A. Ghigo[c], A. Giulietti[a,b], D. Giulietti[a,b,c,h], P. Köster[a,b], T. Levato[a,c], V. Lollo[c], E. Pace[c], N. Pathak[a,h], A. Rossi[d,k], L. Serafini[c,d], G. Turchetti[f,g], C. Vaccarezza[c], P. Valente[i,j], C. Vicario[c] and L.A. Gizzi[a,b,c]

[a]*Intense Laser Irradiation Laboratory, INO, CNR, Pisa, Italy;* [b]*INFN, Sezione di Pisa, Italy;* [c]*INFN, Laboratori Nazionali di Frascati, Italy;* [d]*INFN, Sezione di Milano, Italy;* [e]*Dipartimento di Fisica, Università di Milano-Bicocca, Italy;* [f]*Dipartimento Fisica, Università di Bologna, Italy;* [g]*INFN, Sezione di Bologna, Italy;* [h]*Dipartimento Fisica, Università di Pisa, Italy;* [i]*Dipartimento Fisica, Università di Roma "La Sapienza", Italy;* [j]*INFN, Sezione di Roma 1, Italy;* [k]*Dipartimento Fisica, Università di Milano, Italy*

A 250-TW laser system (FLAME – Frascati laser for acceleration and multidisciplinary experiments) is now in its commissioning phase in a new laboratory at LNF–INFN in the framework of the PLASMONX (Plasma acceleration and monochromatic X-ray generation) project. The laser will deliver <25 fs duration pulses with an energy up to 6 J, at a 10 Hz repetition rate. An *ad hoc* target area has also been designed and is currently being set up, allowing the first test experiments of electron laser wakefield acceleration to be carried out over the next few months in a safe, radiation-protected environment. An overview of the main features of the laser system and target area is given, along with a survey of the design and set-up of the self-injection test experiment, which is expected to reach the production of sub-GeV electron bunches.

Keywords: laser-plasma accelerations; laser wakefield acceleration; Thomson scattering

1. Introduction

The field of electron acceleration via laser–matter interaction, after its first proposal by Tajima and Dawson in 1979 (*1*), has experienced outstanding development in the latter decade, mainly due to the availability of multi-terawatt, ultrashort pulse duration laser systems based on the chirped pulse amplification (CPA) technique (*2*). In particular, laser wakefield acceleration (LWFA) (*1*) has been explored as the most promising technique for the acceleration of electron bunches, which takes advantage of the high longitudinal electric fields supported by electron plasma waves in a plasma. In the LWFA, electrons are trapped in the plasma wave that has a phase velocity very close to the speed of light, and gain energy as long as they are in phase with the accelerating region

---

*Corresponding author. Email: luca.labate@ipcf.cnr.it

ISSN 1042-0150 print/ISSN 1029-4953 online

DOI: 10.1080/10420151003732056
http://www.informaworld.com

of the field (*3*). Recent experiments (*4–6*) show that quasi-monoenergetic electron bunches can be accelerated from the background electron plasma population up to high (>100 MeV) energies. Numerical simulations (*7–9*) show that for sufficiently short and intense laser pulses, the so-called bubble regime of LWFA is activated, in which a single accelerating cavity is produced and effective trapping of electrons occurs. A similar scheme was used in the demonstration of GeV acceleration of electrons (*10*).

The strong convergence of the synchrotron radiation and X-ray free-electron laser community on femtosecond, high field physics, is giving a thrust to the installation of medium- and high-energy laser systems integrated in LINAC and FEL laboratories. The *plasma acceleration and monochromatic X-ray generation* (PLASMONX) project (*11*, *12*), funded by the INFN (Istituto Nazionale di Fisica Nucleare) aims at exploiting the capabilities of an ultrashort pulse duration, sub-PW class laser system and the 10 Hz, 150 MeV SPARC (*13*) linear accelerator based at the LNF (Laboratori Nazionali di Frascati) to explore laser-driven particle acceleration in both the self-injection and the external injection schemes and to study innovative X-ray sources based on Thomson scattering. In this paper, we give an overview of the *Frascati laser for acceleration and multidisciplinary experiments* (FLAME) and we describe the design of a self-injection acceleration test experiment, which has been planned to establish the performances of the FLAME and to assess the degree of control of critical laser parameters.

2. The FLAME and the new laboratory

A new laboratory has been built to host the FLAME at LNF-INFN. The FLAME laboratory includes an ISO7 clean room for the laser system, whose internal layout is shown in Figure 1(a), and a radiation shielded, underground target area, shown in Figure 1(b). Furthermore, the laser pulse can be delivered via a small tunnel intentionally drilled to the bunker where the SPARC linac is hosted and where the external injection electron acceleration and Thomson scattering experiments can be carried out.

The custom-made FLAME (by Amplitude Technologies) is a Ti:Sa, CPA system delivering 20 fs, 800 nm, up to 300 TW laser pulses with a 10 Hz repetition rate at a fundamental wavelength

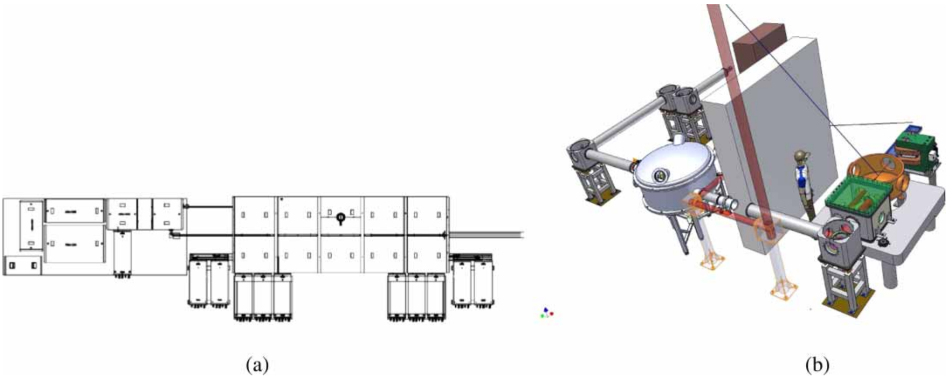
(a) (b)

Figure 1. (a) Schematic layout of the FLAME system; on the left-hand side, the front-end is visible, providing a 600 mJ energy, chirped beam; the beam is then further amplified up to the 7 J level by the cryogenic amplifier stage visible on the right side, pumped by 10 frequency doubled Nd:YAG beams; (b) the chirped (uncompressed) beam is finally sent to a compressor hosted in the underground area (the biggest chamber at the center of the area), where it is compressed down to the ≈ 20 fs duration. The compressed beam can then be transported under vacuum either to the LINAC bunker (transport line on the left side) or to an interaction vacuum chamber in the same area.

of 800 nm. The system features a high, sub-ns contrast ratio ($>10^{10}$) and has a fully remotely controlled operation mode. A general layout of the FLAME system footprint is shown in Figure 1(a). The system includes a front end with pulse contrast enhancement (booster) (*14*, *15*), bandwidth control via DAZZLER (*16*, *17*) and MAZZLER (*18*), a regenerative amplifier, and can yield pulses of 0.7 mJ in an 80 nm bandwidth. These pulses are then further amplified by the first two amplifiers to the 600 mJ level. The third cryogenic amplifier, based upon a 50 mm Ti:Sa crystal, leads to a final energy in the stretched pulses in excess of 6 J. Pulses are then transported in air to the vacuum compressor placed in the underground target area (Figure 1(b)). The final ASE (ns level) contrast of the system is expected to be better than 10^{10}, while the picosecond contrast up to 10 ps before the main pulse is expected to be better than 10^8. Once compressed, the pulse can be transported under vacuum either to the LINAC bunker, for external injection and/or Thomson scattering experiments, or to the self-injection experiment target area shown in Figure 1.

3. Self-injection test experiment

An experiment has been designed and is now in preparation in the underground target area, mainly aiming at assessing the main figures of the laser system by demonstrating the production of high-quality, reproducible electron acceleration in the sub-GeV energy range under controlled interaction conditions. Indeed, as is already known, well-consolidated techniques have been established to measure laser features such as, *e.g.* the temporal contrast, the intensity distribution in the focal spot, the beam pointing stability, and so on. Nevertheless, several constraints do actually apply to some of these techniques in the case of a high energy, ultrashort duration and large aperture beam, as in the FLAME system. It is therefore clear that a correct evaluation of laser performance, including the above parameters, should be carried out “in line”, *i.e.* in operational conditions and at the laser–target interaction point.

In the planned experiment, the main laser pulse will be focused onto a gas-jet target using an $F/10$ off-axis parabola at a maximum intensity above $5 \cdot 10^{19}\,\mathrm{W/cm^2}$ (see Figure 2(a) for a schematic view of the interaction geometry). Several diagnostics are under implementation to investigate the laser–target interaction and accelerated electrons as shown schematically in Figure 2(b). The main optical specifications of these diagnostics were established during previous extensive experimental campaigns (*19–22*) and a pilot experiment recently carried out at the ILIL Laboratory of the CNR in Pisa (Italy). Thomson scattering and Nomarski interferometry are set up perpendicularly to the main laser pulse propagation axis to study and characterize ionization and basic laser–plasma interaction issues. A second group of diagnostics, including scintillators coupled to photomultipliers, a phosphor screen (LANEX), a custom (*23*), dose-sensitive, radiochromic film stack, enables indirect and direct detection and characterization of the accelerated electron bunches. Moreover, a magnetic spectrometer is currently being developed, which will provide a better than 10% energy resolution for an electron energy range up to about 1 GeV.

In what follows, we present some results from the simulations of the gas ionization by the laser pulse and a PIC simulation of the pulse interaction with the plasma.

3.1. *Modelling of ionization*

We have performed a numerical simulation to gain quantitative information about the electron density evolution and its effect on the laser pulse. The simulation is based on a tunnel ionization model (*24*). Our code calculates the rate of tunnel ionization in a non-adiabatic regime, *i.e.* as a function of the instantaneous laser phase. According to this model, the rate of ionization is given as follows: $\Gamma = N(t)\exp[-(E^2 f^2(t)/\omega_{\mathrm{L}}^3)\phi(\gamma,\theta)]$, where E is the laser electric field amplitude,

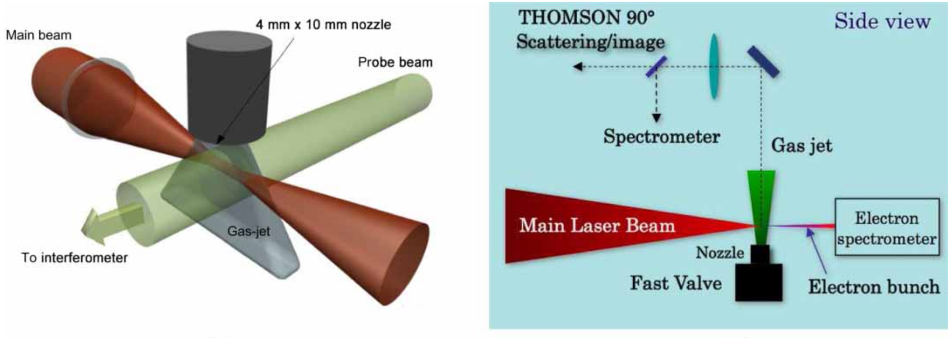

(a) (b)

Figure 2. Interaction geometry for the self-injection test experiment (a) and schematic layout of the main diagnostics (b).

$f(t)$ the pulse envelope, and ω_L the laser frequency. In the above equation, the term $\phi(\gamma, \theta)$ includes the dependence upon the Keldysh parameter γ, the ionization potential I_p, the average energy of electron oscillations in the laser field U_p, and the phase of the laser field θ.

In the simulation discussed below, a laser pulse with the time profile shown in Figure 3(a) was focused at the center of a step-like uniform density profile of the neutral gas medium. The maximum neutral atomic density was set to $1.5 \cdot 10^{18}$ W/cm^2. The intensity profile of the Gaussian beam had a spatial dependence of the form $I = I_0(w_0^2/w(z)^2)\exp[-2(r^2/w(z)^2)]$, where $w(z)$ is the spot size as a function of propagation distance, including the M^2 factor for our real beam. Simulations were performed for helium and nitrogen gases. The input laser parameters in the code were as follows: pulse duration 30 fs, energy 5 J, peak power 166 TW, spot size = 9 µm, intensity = $6.54 \cdot 10^{19}$ W/cm^2, $a_0 = 5.5$, Rayleigh range 141.37 µm, $M^2 = 1.5$. The population of electrons is then computed from the rate equations, neglecting recombination.

We studied the effect of the picosecond precursor to the main pulse, as measured for the FLAME system by the manufacturing company. In detail, the contrast up to 10 ps before the main pulse is expected to be better than 10^8, which corresponds to a precursor intensity in the focal spot below $5 \cdot 10^{11}$ W/cm^2. It can be shown that this intensity produces a negligible ionization in the gas, if any, and gives no significant contribution to the interaction dynamics. On the other hand, for times before the main pulse smaller than 10 ps, the intensity is expected to increase up to 10^{-5} of the peak intensity. It is therefore interesting to evaluate the effect of this laser intensity on the gas in the focal region. We modelled this case, taking a simplified intensity profile as the one plotted in Figure 3(a) and assuming a level for the intensity of the picosecond pedestal of $3 \cdot 10^{-5}$ times the peak intensity. The color map of Figure 3(b) (color online only) shows the result of the calculation. According to this plot, the precursor picosecond pulse gives rise to a narrow channel of partial ionization along the axis of the propagation of the laser pulse. This effect was clearly

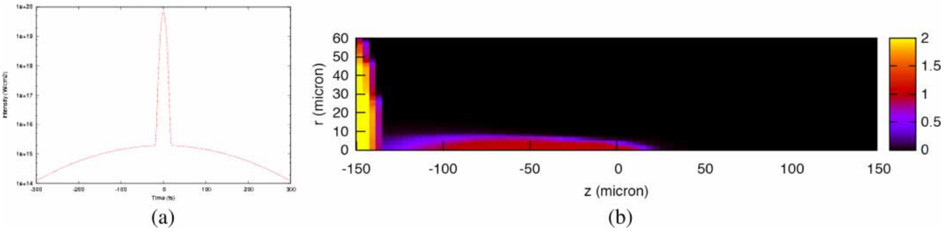

(a) (b)

Figure 3. (a) Simplified intensity profile used to estimate the effect on the gas of a precursor radiation in the focal spot in the picosecond time domain as expected for the FLAME system. (b) Color map (online only) showing the ionization induced in the gas by the laser pulse as shown on the left.

observed in a previous experiment (*25*) carried out at moderately relativistic intensities, using femtosecond plasma interferometry. In that study, it was shown that this precursor ionization acts on the main pulse mainly via refraction, and no evidence was found of detrimental effects on a stable propagation. In fact, the presence of a precursor ionization may initiate a channelling process that may support propagation for longer distances than that set by focusing optics. These circumstances will be verified using high resolution, femtosecond interferometry.

3.2. *PIC simulations of the electron self-injection and acceleration*

As anticipated above, the ultimate goal of the self-injection test experiment is the production of sub-GeV-class electron bunches from laser–plasma interaction using a gas-jet of a few millimeters, without external guiding for the laser, entering directly into the so-called "bubble regime" (*26, 27*). In the bubble regime, a short ($c\tau < \lambda_p/2$) and intense ($a_0 > 2$) laser pulse expels the plasma electrons outward, creating a bare ion column. The blown-out electrons form a narrow sheath outside the ion channel and the space charge generated by the charge separation pulls the electrons back, creating a bubble-like wake. For sufficiently high laser intensities, ($a_0 > 3.5/4$) electrons at the back of the bubble can be injected into the cavity, where the longitudinal accelerating field is of the order of $\sim 100\sqrt{n(\mathrm{cm}^{-3})}\,\mathrm{V/m}$.

The FLAME meets both conditions of short pulse length and high intensity. The working point we have considered for our experiment is given by the following parameters: gas jet length $L_{\text{gas jet}} = 4\,\mathrm{mm}$ (Figure 3(a)), electron density $n_e = 3 \cdot 10^{18}\,\mathrm{W/cm}^3$, pulse duration $\tau = 30\,\mathrm{fs}$, maximum intensity $I_0 = 5.2 \cdot 10^{19}\,\mathrm{W/cm}^2$ and waist size $w_0 = 16\,\mu\mathrm{m}$. In this case, following the phenomenological description given in (*28*), we expect to obtain a quasi-monochromatic (few % momentum spread) bunch with a charge of ~0.6 nC and an energy of approximately 1.0 GeV after 4 mm. The acceleration process has also been investigated through 3D particle-in-cell (PIC) simulations performed with the fully self-consistent, relativistic, electromagnetic code ALaDyn (*29, 30*). The results are summarized in Figure 4, where we show the electron density and energy spectrum at the time when the pulse has gone through the whole plasma length. At the end of the simulation, a bunch with an energy of 0.9 GeV and a momentum spread (rms) of 3.3% is obtained; the charge is 0.6 nC, the bunch length 1.8 μm (average current ~50 kA), and the beam divergence (rms) 2.8 mrad. The results are in good agreement with Lu et al. (*28*).

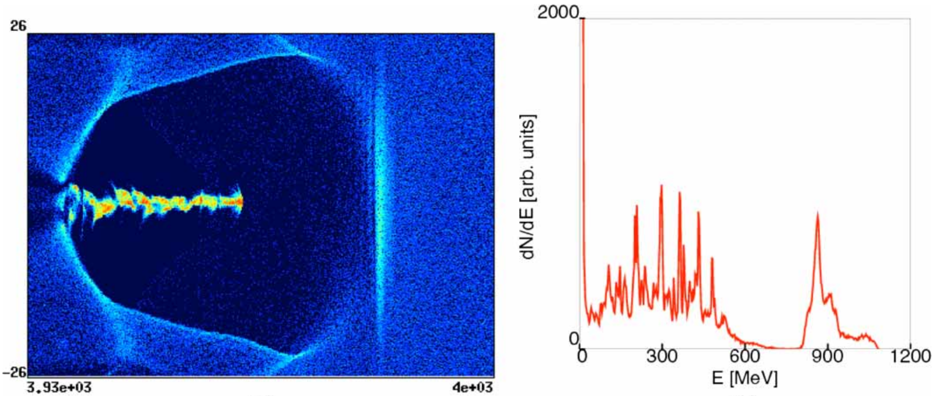

(a) (b)

Figure 4. Electron density map (a) and energy spectrum (b) as obtained from the 3D PIC simulation of the self-injection test experiment.

4. Summary and conclusions

A new high-power, sub-GeV, ultrashort duration laser system is now in an advanced commissioning phase at LNF–INFN, where a new laboratory, close to an existing 150 MeV LINAC laboratory, has been established. This new installation will allow a wide range of novel experiments to be carried out, based on the combined use of high-quality electron bunches and ultrashort and ultraintense laser pulses. Experimental schemes which can be foreseen to be feasible in the new laboratory include self- and external injection electron acceleration based on the LWFA scheme as well as monochromatic and tunable X-ray radiation production based upon Thomson scattering. More advanced experiments, such as the production of X-ray generation by all-optical schemes, could be performed as well. A first experiment is now in an advanced phase of preparation and has been discussed, mainly devoted to assessing the laser system figures by producing high-quality, sub-GeV electron bunches produced by a self-injection LWFA scheme.

Acknowledgements

The PLASMONX project is funded by INFN. The activity described here is also supported by the MIUR SPARX/C projects and by the MIUR-FSSRIS project “Impianti innovativi multiscopo per la produzione di radiazione X”.

References

(1) Tajima, T.; Dawson, J.M. *Phys. Rev. Lett.* **1979,** *51,* 267–270.
(2) Strickland, D.; Moureau, G. *Opt. Commun.* **1985,** *56,* 219–221.
(3) Esarey, E.; Sprangle, P.; Krall, J.; Ting, A. *IEEE Trans. Plasma Sci.* **1996,** *24,* 252–288.
(4) Faure, J.; Glinec, Y.; Pukhov, A.; Kiselev, S.; Gordienko, S.; Lefebvre, E.; Rousseau, J.-P.; Burgy, F.; Malka, V. *Nature* **2004,** *431,* 541–544.
(5) Malka, V.; Faure, J.; Glinec, Y.; Pukhov, A.; Rousseau, J.-P. *Phys. Plasmas* **2005,** *12,* 056702-1–8.
(6) Faure, J.; Glinec, Y.; Gallot, G.; Malka, V. *Phys. Plasmas* **2006,** *13,* 056706-1–12.
(7) Pukhov, A.; Kiselev, S.; Kostyukov, I.; Shorokhov, O.; Gordienko, S. *Nucl. Fusion* **2004,** *44,* S191–S201.
(8) Pukhov, A.; Gordienko, S.; Kiselev S.; Kostyukov, I. *Plasma Phys. Control. Fusion* **2004,** *46,* B179–B186.
(9) Kostyukhov, I.; Pukhov, A.; Kiselev, S. *Phys. Plasmas* **2004,** *11,* 5256–5264.
(10) Leemans, W.P.; Nagler, B.; Gonsalves, A.J.; Toth, C.; Nakamura, K.; Geddes, C.G.R.; Esarey, E.; Schroeder, C.B.; Hooker, S.M. *Nat. Phys.* **2006,** *2,* 696–699.
(11) PLASMONX Project Webpage. http://www.lnf.infn.it/acceleratori/plasmonx/.
(12) Gizzi, L.A.; Bacci, A.; Betti, S.; Cecchetti, C.A.; Ferrario, M.; Gamucci, A.; Giulietti, A.; Giulietti, D.; Koester, P.; Labate, L.; Levato, T.; Petrillo, V.; Serafini, L.; Tomassini, P.; Vaccarezza, C. *Europ. Phys. J. Spec. Topics* **2009,** *175,* 3–10.
(13) Alesini, D.; Bertolucci, S.; Biagini, M.E.; Biscari, C.; Boni, R.; Boscolo, M.; Castellano, M.; Clozza, A.; Di Pirro, G.; Dargo, A.; Esposito, A.; Ferrario, M.; Fusco, V.; Gallo, A.; Guiducci, S.; Incurvati, M.; Laurelli, P.; Ligi, C.; Marcellini, F.; Migliorati, M.; Milardi, C.; Palumbo, L.; Pellegrino, L.; Preger, M.; Raimondi, P.; Ricci, R. Sanelli, C.; Sgamma, F.; Spataro, B.; Serio, M.; Stecchi, A.; Stella, A.; Tazzioli, F.; Vaccarezza, C.; Vescovi, M.; Vicario, C.; Zobov, M.; Acerbi, E.; Alessandria, F.; Barni, D.; Bellomo, G.; Boscolo, I.; Broggi, F.; Cialdi, S.; Demartinis, C.; Giove, D.; Maroli, C.; Petrillo, V.; Rome, M.; Serafini, L.; Chiadroni, E.; Felici, G.; Levi, D.; Mastrucci, M.; Mattioli, M.; Medici, G.; Petrarca, G.S.; Catani, L.; Cianchi, A. *Nucl. Instrum. Methods A* **2003,** *507,* 345–349.
(14) Itatani, J.; Faure, J.; Nantel, M.; Mourou, G.; Watanabe, S. *Opt. Commun.* **1998,** *148,* 70–74.
(15) Nantel, M.; Itatani, J.; Tien, A.-C.; Faure, J.; Kaplan, D.; Bouvier, M.; Buma, T.; Van Rompay, P.; Nees, J.; Pronko, P.P.; Umstadter, D.; Mourou, G.A. *IEEE J. Sel. Top. Quantum Electron.* **1998,** *4,* 449–458.
(16) Verluise, F.; Laude, V.; Cheng, Z.; Spielmann, C.; Tournois, P. *Opt. Lett.* **2000,** *25,* 575–577.
(17) Verluise, F.; Laude, V.; Huignard, J.P.; Tournois, P.; Migus, A. *J. Opt. Soc. Am. B* **2000,** *17,* 138–145.
(18) Oksenhendler, T.; Kaplan, D.; Tournois, P.; Greetham, G.M.; Estable, F. *Appl. Phys. B* **2006,** *83,* 491–494.
(19) Giulietti, D.; Galimberti, M.; Giulietti, A.; Gizzi, L.A.; Borghesi, M.; Balcou, Ph.; Rousse, A.; Rousseau, J.-Ph. *Phys. Rev. E* **2001,** *64,* 015402-1–4.
(20) Gizzi, L.A.; Galimberti, M.; Giulietti, A.; Giulietti, D.; Köster, P.; Labate, L.; Tomassini, P.; Martin, Ph.; Ceccotti, T.; D’Oliveira, P.; Monot, P. *Phys. Rev. E* **2006,** *74,* 036403-1–5.
(21) Giulietti, A.; Bourgeois, N.; Ceccotti, T.; Davoine, X.; Dobosz, S.; D’Oliveira, P.; Galimberti, M.; Galy, J.; Gamucci, A.; Giulietti, D.; Gizzi, L.A.; Hamilton, D.J.; Lefebvre, E.; Labate, L.; Marquès, J.R.; Monot, P.; Popescu, H.; Réau, F.; Sarri, G.; Tomassini, P.; Martin, P. *Phys. Rev. Lett.* **2008,** *101,* 105002-1–4.
(22) Gizzi, L.A.; Betti, S.; Galimberti, M.; Giulietti, A.; Giulietti, D.; Labate, L.; Levato, T.; Tomassini, P.; Monot, P.; Ceccotti, T.; D’Oliveira, P.; Martin, P. *Phys. Rev. E* **2009,** *79,* 056405-1–6.

(23) Galimberti, M. *J. Opt. Soc. Am. A* **2007,** *24,* 304–310.
(24) Yudin, G.L.; Ivanov, M. *Phys. Rev. A* **2001**, *64,* 013409-1–4.
(25) Giulietti, A.; Tomassini, P.; Galimberti, M.; Giulietti, D.; Gizzi, L.A.; Köster, P.; Labate, L.; Ceccotti, T.; D'Oliveira, P.; Auguste, Th.; Monot, P.; Martin, Ph. *Phys. Plasmas* **2006,** *13,* 093103-1–6.
(26) Pukhov, A.; Meyer-ter-Vehn, J. *Appl. Phys. B* **2002,** *74,* 355–361.
(27) Gordienko, S.; Pukhov, A. *Phys. Plasmas* **2005,** *12,* 043109-1–11.
(28) Lu, W.; Tzoufras, M.; Joshi, C.; Tsung, F.S.; Mori, W.B.; Vieira, J.; Fonseca, R.A.; Silva, L.O. *Phys. Rev. Spec. Top. Accel. Beams* **2007,** *10,* 061301-1–12.
(29) Benedetti, C.; Sgattoni, A.; Turchetti, G.; Londrillo, P. *IEEE Trans. Plasma Sci.* **2008,** *36,* 1790–1798.
(30) Benedetti, C.; Londrillo, P.; Petrillo, V.; Serafini, L.; Sgattoni, A.; Tomassini, P.; Turchetti, G. *Nucl. Instrum. Methods A* **2009,** *608,* S94–S98.